

# Overcoming Large-Scale Fading in Cellular Systems With Network Coordination



# Overcoming Large-Scale Fading in Cellular Systems With Network Coordination

Dushyantha A. Basnayaka, *Member, IEEE*, and Harald Haas, *Member, IEEE*

***Abstract*—The cellular systems with network coordination are known for increasing the cell edge user throughput by processing signals captured by geographically distributed base stations coherently. This concept is also known as macrodiversity or coordinated multipoint (CoMP) in the literature. It is now well known that large-scale fading has a significant influence on the link-level performance of users in multiuser (MU) multicell systems. In this paper, we investigate a channel distribution information (CDI)-based MU multiple-input–multiple-output (MIMO) power control problem in the uplink with joint processing to overcome the large-scale fading in macrodiversity systems. There are many power control algorithms for different variants of this problem, but the CDI-based problem in MU scenario has not been well addressed in the literature. Perhaps, the lack of understanding of the performance of macrodiversity MU systems, in terms of CDI, may have prohibited advanced power control solutions. Despite such analytical difficulties, we propose a simple algorithm for this uplink power control problem, and its accuracy is proved using Monte Carlo simulation.**

***Index Terms*—Power control, CoMP, uplink, network MIMO, CDI, CSI, large scale fading, symbol error rates.**

## I. Introduction

NETWORK coordination is a novel concept for exploiting the out-of-cell interference in dense small cell deployments where performance is mainly governed by the interference originating from nearby cells [1]–[3]. In cellular systems with network coordination, geographically distributed base stations (BSs) capture independently faded replicas of data signals from users and process them coherently to suppress interference, and this is often considered with multiple users [4]. This concept has been a research topic for some time. However, it is formally recognized after it is adopted as a candidate technology for 3rd generation partnership project (3GPP) long term evolution-advanced (LTE-A) standards recently [5]. This technology is interesting not only because it holds the potential for significant capacity gains, but also poses some unprecedented theoretical challenges. Among many theoretical challenges, perhaps the most fundamental challenge is understanding how performance varies with the macrodiversity power profile. A good comparison between denser deployments and coordination is given in [6]. On the other hand, uplink power control is also a well-established method to achieve a predefined quality, minimize interference to other users in the system and optimally utilize energy of the mobile terminal in cellular systems [7]. The system controls the power of its transmitters in such a way that interference caused to neighboring cells is minimal while maintaining satisfactory signal-to-interference-plus-noise (SINR) level at the desired BS. Initially, power control is proposed to single-input single-output (SISO) cellular systems [8], [9], but currently results are available for multiple-input-multiple-output (MIMO) cellular systems [10]. The network coordination in conjunction with power control can increase the system throughput even further while guaranteeing minimal energy consumption.

In coordinated multiuser (MU) multi-cell systems, the large scale fading plays a critical role [11]. The links between users and BSs have very different large-scale fading due to geographical separation of BSs. Therefore, it is more important to manage large-scale fading in multi-cell systems than in single-cell systems. In this work, we utilize a power control scheme to overcome the large-scale fading effect. Hence, it is based on channel distribution information (CDI). In other words the transmitters only adapt to the slow fading. In this paper, CDI is defined as the average link gains due to large-scale channel impairments such as path loss and shadowing. In many existing works on power control, single-cell systems and instantaneous channel state information (CSI) are assumed. The CDI based power control methods may be very useful in practice over CSI based methods due to several reasons. In instantaneous CSI scenarios, when CSI changes the power levels have to be revised. In order to circumvent such computational burden and to reduce the frequency of power updates, we can resort to adjusting the transmit power based on CDI. This approach will be more beneficial for macrodiversity systems especially in high user mobility environments. The channel coefficients change too quickly to be accurately measured and fed back to the users in high mobility users. Therefore, instead of adjusting the transmit power levels of users to erroneous and/or delayed CSI, users can rely on relatively more accurate large-scale fading coefficients. Furthermore, CDI based power control can be used to overcome the so-called *near-far-problem* in cellular wireless uplink [12, Section 15.5.3].

In this paper, we formulate a systematic solution to employ power control for macrodiversity MU systems using CDI. In particular, our system of interest is a multi-cell wireless uplink system with distributed users in the coverage area communicating with geographically distributed BSs in the same *time and frequency* resource. We assume BSs are connected to a

Manuscript received September 3, 2013; revised January 24, 2014 and April 12, 2014; accepted May 17, 2014. Date of publication May 30, 2014; date of current version July 18, 2014. The work of H. Haas was supported by the Engineering and Physical Sciences Research Council (EPSRC) under Established Career Fellowship Grant EP/K008757/1. The editor coordinating the review of this paper and approving it for publication was D. I. Kim.

The authors are with the Institute for Digital Communications, University of Edinburgh, Edinburgh EH9 3JL, U.K. (e-mail: d.basnayaka@ed.ac.uk).

Color versions of one or more of the figures in this paper are available online at http://ieeexplore.ieee.org.

Digital Object Identifier 10.1109/TCOMM.2014.2327099

backhaul processing unit (BPU) for facilitating the joint processing (JP). This setting effectively creates a virtual MU-MIMO multiple access channel (MAC). Therefore, theoretically existing power control algorithms for single-cell MU systems which adapt to the instantaneous CSI can be applied to this problem. If we envision a power control mechanism based on CDI, the fact that every link between users and BSs experience very different large-scale fading should be carefully handled. In addition, power control algorithms for uplink MU coordinated multi-point (CoMP) systems must account the fact that co-scheduled users are decoded using some form of multiuser detection [13]. As a result the uplink power control should be done cooperatively. However, the existing methods do not seem to address this problem fully [14]–[16]. It is a challenging question how to combine received signals from multiple geographically distributed BSs to form the optimal detection of transmitted signals from any user. In [11], authors analytically show that the large scale fading has a complex effect on the link-level performance of users in MU systems. In [15], [17], a heuristic performance measure is proposed by simply adding up received SINR at individual BSs and the power allocation scheme is determined by optimizing this metric (see eq. (18)). It appears that their performance measure is chosen based on basic SINR concepts. Its underlying functional links to average error probability, capacity are not clear. These metrics are crude approximations and not rigorously derived (see Section V-A). Therefore, it is difficult to guarantee that macrodiversity systems will achieve intended performance if power allocation schemes utilize those performance metrics (see Fig. 6). A more complex and analytical analysis is provided in [11], where several new systematic performance metrics are proposed in terms of CDI. Due to these analytical developments in the area of macrodiversity MU multi-cell systems with JP, in this paper we propose a new uplink power control solution systematically using CDI, where analytically proved advanced performance metrics are employed.

The rest of the paper is laid out as follows. Section II provides the motivation behind this work. Section III describes the system model in detail. The main analysis is presented in Section V. Sections VI and VII give numerical results and important remarks on CDI based power control, respectively. Finally, Section VIII summarizes the main results of the paper.

## II. Motivation

In this paper we consider a CoMP system with multiple distributed users. However, in this section a motivational example which presents the conceptual background behind the current work is provided. We consider an isolated cell with a single antenna BS in the center of the cell, and $K$ single antenna users in the cell coverage. The complex baseband channel model in the uplink can be written as

$$r_k = h_k x_k + n_k, \quad \text{for} \quad k = 1, \ldots, K, \tag{1}$$

where $x_k \in \mathcal{C}$ is the transmitted signal and $r_k \in \mathcal{C}$ is the received signal by the user $k$. The $n_k \in \mathcal{C}$ is the additive-white-Gaussian-noise (AWGN) with variance $\sigma^2$. We assume that $x_k$ has a transmit power constraint, i.e., $\mathcal{E}\{|x_k|^2\} = d_k$ and in Rayleigh fading, $h_k \sim \mathcal{CN}(0, P_k)$, where $h_k$ is the channel coefficient between user k and the BS antenna. Here $\mathcal{E}\{.\}$, and $\mathcal{CN}(0, \tau)$ denote the expectation operator and zero mean complex normal distribution with variance $\tau$ respectively. The $P_k$ is referred as the average link power (or gain) due to both the path loss and the shadowing. This represents a wireless system with non-homogeneous users. It is further assumed that at any time, the system chooses one out of $K$ users for communication so they do not interfere each other. In order to achieve uniform level of performance for majority of users by overcoming near-far problem, and to save power at the user terminal, it is a well-known practice to use uplink power control. This may be accomplished in two different ways. The first obvious method is using instantaneous CSI for power control but if system prefers reduced frequency of power control feedback to users, BS can apply power control to overcome large-scale fading, hence, $P_k$ is assumed constant in the channel model. Here, we further assume slow fading information is fed back to the mobile users, so transit power levels can be revised accordingly. In this case, the $k$th user may use the following simple power control scheme

$$d_k = \min\left(U_k, \frac{\sigma^2 T_0}{P_k}\right), \tag{2}$$

where $T_0$ is a fixed desired signal-to-noise-ratio (SNR) at the BS before receive processing and $U_k$ is a fixed transmit power constraint for user $k$. Since, single antenna users communicate with a single antenna BS with no interference, the link-level performance of users depends on the average receive SNR which is defined by $d_k P_k/\sigma^2$ for $\forall\, k$. This should explain the simple power control scheme in (2). The picture is not that clear when there are multiple antennas at the BS and multiple users use the same channel. It is not clear how to combine received signals from multiple antennas to form an optimal performance metric in terms of CDI for transmitted signals from any user. The complexity grows further for systems where there are multiple distributed BSs in MU scenario which is the case in CoMP systems for LTE-A standards. In this paper however, we solve this problem and provide a rich set of tools to devise such power control schemes for many wireless communication scenarios where network coordination will be used.

## III. System Model

We consider a macrodiversity MU-MIMO uplink communication system in Rayleigh fading with $M$ BSs and $N$ distributed users. Each BS may have multiple antennas. Therefore, we assume there are $n_R$ number of antennas in total at the receive end. We further assume single antenna users. This specifications create a virtual MIMO link of $n_R \times N$ dimension. By adopting the well-established complex baseband mathematical model, the receive vector $\boldsymbol{r}$ is given by [4]

$$\boldsymbol{r} = \sum_{k=1}^{N} \sqrt{d_k}\boldsymbol{h}_k s_k + \boldsymbol{n}, \tag{3}$$

$$= \boldsymbol{H} D^{\frac{1}{2}} \boldsymbol{s} + \boldsymbol{n}, \tag{4}$$

where $\mathcal{C}^{N\times 1}$ vector $\boldsymbol{s} = (s_1, \ldots, s_N)$ is the transmitted data signal, $\mathcal{C}^{n_R \times N}$ matrix, $\boldsymbol{H} = \{\boldsymbol{h}_1, \boldsymbol{h}_2, \ldots, \boldsymbol{h}_N\}$ is the channel

matrix which captures the fading between users and the BS antenna array, and $\boldsymbol{n}$ is the $\mathcal{C}^{n_R\times 1}$ AWGN vector with independent entries with $\mathcal{E}\{|n_i|^2\}=\sigma^2$, for $i=1,2,\ldots,n_R$. The $\mathcal{C}^{N\times N}$ diagonal matrix, $\boldsymbol{D}=\mathrm{diag}(d_1,d_2,\ldots,d_N)$ represents the power control matrix. It is convenient to define the power loading vector, $\boldsymbol{d}$ as $\boldsymbol{d}=(d_1,d_2,\ldots,d_N)$. Furthermore, we assume that transmit data signals are normalized to give $\mathcal{E}\{|s_k|^2\}=1$, for $k=1,2,\ldots,N$. The channel matrix $\boldsymbol{H}$ contains independent elements, $h_{ik}\sim\mathcal{CN}(0,P_{ik})$ which represents the complex channel gain between user $k$ and BS antenna $i$, where $\mathcal{E}\{|h_{ik}|^2\}=P_{ik}>0\ \ \forall i,k$. We define the $\mathcal{C}^{n_R\times N}$ macrodiversity power profile matrix, $\boldsymbol{P}=\{P_{ik}\}$, which holds the average link powers due to shadowing and path loss to facilitate our subsequent mathematical manipulations. We let $P_{ik}$ be given by

$$P_{ik}=A\Psi_{ik}\left(\frac{r_0}{r_{ik}}\right)^{\gamma}, \tag{5}$$

where $r_{ik}$ is the distance between the $k$th mobile and the $i$th BS antenna, $r_0$ is a fixed reference distance, $\gamma$ is the pathloss coefficient, and $\Psi_{ik}$ is the log-normal shadowing with standard deviation $\sigma_{SF}$ between the $k$th mobile and the $i$th BS. The constant $A$ is a scaling parameter which guarantees that links have acceptable SNR at a reference distance, $r_0$. Note that the pathloss and shadowing model in (5) can be used to model many practical large scale fading scenarios and the values for $A$, $r_0$, and $\gamma$ can be calculated numerically to approximate empirical measurements [18].

In this MU multi-cell system, we assume that BPU knows CDI: $\boldsymbol{P}$ perfectly. Since users are assumed to adapt their transmit power levels to slow fading only, the BPU calculates the transmit power levels based on $\boldsymbol{P}$ and feeds back resultant $d_k$s to relevant mobile users, so transit power levels can be revised accordingly. Note here that $d_k$s are functions of $\boldsymbol{P}$ matrix only. Due to the shadowing effect, slow fading may still change at a time horizon of seconds, which is larger than fast fading but can still happen within the same cell coverage area. The users transmit their data signals at revised power levels. In this way, users can *cooperatively* overcome large-scale fading. At the BPU, the received signal vector is linearly transformed into an estimate upon which the system makes a hard decision on the transmitted signal vector. In this work, we assume that the BPU uses minimum-mean-squared-error (MMSE) receive combining to suppress the multiple access interference [19]. The combiner output vector becomes

$$\tilde{\boldsymbol{s}}=\boldsymbol{W}^H\boldsymbol{r}, \tag{6}$$

where $\mathcal{C}^{n_R\times N}$ matrix $\boldsymbol{W}$ is the weight matrix. The MMSE receive beamforming matrix in JP MMSE is given by

$$\boldsymbol{W}=\left(\boldsymbol{H}\boldsymbol{H}^H+\sigma^2\boldsymbol{I}_{n_R}\right)^{-1}\boldsymbol{H}. \tag{7}$$

Thus, the combiner output SINR of the $k$th user is well-known and is given by

$$Z_k=\boldsymbol{h}_k^H\boldsymbol{R}_k^{-1}\boldsymbol{h}_k,\quad \forall k, \tag{8}$$

where $\mathcal{C}^{n_R\times 1}$ vector, $\boldsymbol{h}_k$ is the $k$th column of $\boldsymbol{H}$ and $\boldsymbol{R}_k=\sum_{u\neq k}^{N}\boldsymbol{h}_u\boldsymbol{h}_u^H+\sigma^2\boldsymbol{I}$ [20]. The statistical performance of $Z_k$ is well-known for co-located antenna arrays at BS end but it is a very difficult problem for distributed antennas case. However, it has been shown that the probability density function (PDF) of $Z_k$ can be approximated by a mixture of exponentials [11]. There are $n_R$ exponential terms in the approximation (see Section VI of [11]). Many performance metrics can be derived using these PDF results. For instance, the average symbol error rate (SER) of user $k$ can be given for many modulation schemes ([12, Table 6.1]) as

$$\mathrm{SER}_k=\mathcal{E}_{\boldsymbol{H}}\left\{aQ(\sqrt{2gZ_k})\right\}, \tag{9}$$

where $Q(x)=(1/\sqrt{2\pi})\int_x^{\infty}e^{-(t^2/2)}dt$ is the Gaussian Q-function defined in [23], and $a$, and $g$ are constants. The desired result can be obtained by evaluating the expectation in (9) using the PDF results in [11]. See more details in Section V-B. Here the average SER is only averaged over the fast fading. Hence, we may also called it local average SER henceforth.

## IV. Preliminaries

This work, and several previous work have shown that there is a strong functional link between matrix permanents and the link level performance of macrodiversity MU-MIMO systems [11], [21]. Therefore, a brief description on matrix permanents is provided as follows. A formal definition for the matrix permanent is found in [22]. Let $\boldsymbol{B}=(b_{ik})$ be an $m\times n$ matrix with $m\geq n$. The permanent of $\boldsymbol{B}$, written $\mathrm{Perm}(\boldsymbol{B})$ (also $\mathrm{perm}(\boldsymbol{B})$ when $m=n$), is defined by

$$\mathrm{Perm}(\boldsymbol{B})=\sum_{\sigma}b_{1,\sigma_1}b_{2,\sigma_2}\ldots b_{n,\sigma_n}, \tag{10}$$

where the summation extends over all one-to-one functions from $\{1,\ldots,n\}$ to $\{1,\ldots,m\}$. The sequence $(b_{1,\sigma_1}b_{2,\sigma_2}\ldots b_{n,\sigma_N})$ is called a diagonal of $\boldsymbol{B}$, and the product $b_{1,\sigma_1}b_{2,\sigma_2}\ldots b_{n,\sigma_N}$ is a diagonal product of $\boldsymbol{B}$. Thus the permanent of $\boldsymbol{B}$ is the sum of all diagonal products of order $n$ of $\boldsymbol{B}$. For instance, let $\boldsymbol{B}$ be

$$\boldsymbol{B}=\begin{pmatrix}a\\b\\c\end{pmatrix}. \tag{11}$$

The permanent of matrix $\boldsymbol{B}$, becomes,

$$\mathrm{Perm}(\boldsymbol{B})=a+b+c, \tag{12}$$

and if $\boldsymbol{B}$ be

$$\boldsymbol{B}=\begin{pmatrix}a&b\\c&d\\e&f\end{pmatrix}, \tag{13}$$

the $\mathrm{Perm}(\boldsymbol{B})$ becomes,

$$\mathrm{Perm}(\boldsymbol{B})=ad+af+cb+cf+ed+eb. \tag{14}$$

Unlike determinant, matrix permanent is defined for both rectangular and square matrices. Furthermore, the summation for the matrix permanent of a real $m\times n$ $(m>n)$ rectangular

matrix with no duplicate columns and rows has $m!/(m-n)!$ terms, hence, $(m!/(m-n)!)(n-1)$ multiplications and $(m!/(m-n)!)-1$ summations.

## V. Uplink Power Control

In this section we briefly review the existing power control methodologies for macrodiversity MIMO systems and present the main algorithm of this paper in detail. There are two main uplink power control approaches for cellular systems. The first is maximizing an objective function for a given maximum or average transmit power limit. The most common objective function is the sum capacity or weighted sum capacity [24]. The next is minimizing the transmit power while guaranteeing certain quality of service (QoS) thresholds. The SINR is used in many cases as the QoS function [9].

### A. Review of Existing Performance Metrics

In contrast to the single cell systems, devising an appropriate performance measure in terms of CDI is a very difficult problem for macrodiversity MU-MIMO systems. We consider the channel equation in (3), and the received signal by the $i$th BS antenna is given by

$$r_i = \sum_{k=1}^{N} \sqrt{d_k} h_{ik} s_k + n_i, \quad \text{for} \quad \forall\, i. \tag{15}$$

The goal here is devising an appropriate performance measure for the user $k$ in terms of CDI. It is clear from (7) that all $r_i$s are combined in a complex manner. In [15], authors assume the sum local average received power from user $k$ at all BS antennas ignoring interference power is an appropriate measure for the performance of user $k$. It suggests the following SNR metric for user $k$:

$$\text{SNR}_k = \frac{d_k}{\sigma^2} \left( \sum_{i=1}^{n_R} P_{ik} \right) \quad \forall\, k. \tag{16}$$

It is clear that the performance metric in (16) is based on rather instinctive assumption. Furthermore, in [15], authors suggest a power control method to overcome the large scale fading as follows.

$$d_k = \frac{\sigma^2 T_0}{\sum_{i=1}^{n_R} P_{ik}}, \quad \forall\, k, \tag{17}$$

where $T_0$ in macrodiversity case, is the average target received power by all BSs before receive combining. The design goal here is to make the post combining performance comparable by making sure the average received power before receive combining is the same. However, in [11] it has been shown that such behavior can not be guaranteed (see Section II). In another contribution, the following SINR metric is considered [17]:

$$\text{SINR}_k = \sum_{i=1}^{n_R} \frac{d_k P_{ik}}{\sum_{u \neq k}^{N} d_u P_{iu} + \sigma^2}, \quad \forall\, k. \tag{18}$$

Clearly the metric in (18) takes a major step forward by including the average interference power into the performance metric. However, it also seems here that the average signal-to-interference-plus-noise ratio of user $k$ at each receive antenna:

$$\text{SINR}_k^i = \frac{d_k P_{ik}}{\sum_{u \neq k}^{N} d_u P_{iu} + \sigma^2}, \quad \forall i, k, \tag{19}$$

is simply summed up to obtain the final SINR metric. There are a few more contributions where similar metrics are used for managing interference through power control [25], [26]. The performance metrics which we discuss here are sensible choices but appear insufficient to capture the performance accurately (see Fig. 6). Therefore, we need a good compromise which has both accuracy and tractability. A more complex and analytical analysis for the performance of MU multi-cell MIMO systems is provided in [11] where a strong functional link between the link-level performance and the large-scale fading is uncovered. Moving away from traditional metrics which are broadly based on basic SINR concepts, in this paper, we employ latest developments in the field for devising a novel power control algorithm.

### B. Proposed Algorithm

Our algorithm targets at minimizing transmit power while guaranteeing certain QoS thresholds for each user in the macrodiversity MU-MIMO system. The QoS metric is chosen to be the uncoded average SER.[1] The local average SER of the $k$th user for $M$-PSK and $M$-QAM type modulation schemes can be evaluated as

$$\text{SER}_k = a \int_0^T Q(\sqrt{2gz}) f_{Z_k}(z) dz, \tag{20}$$

where $g$ is a function of the modulation order, $M$ and $T = \pi/2$. From [11], the PDF of $Z_k$ is approximately given by

$$f_{Z_k}(z) \approx \frac{\Delta_k(\bar{\boldsymbol{Q}}_k, \bar{\gamma})}{|\boldsymbol{P}_k| d_k^L} \sum_{\ell=1}^{n_R} \eta_\ell e^{-\omega_\ell z}, \quad \forall\, k, \tag{21}$$

where $\Delta_k(\bar{\boldsymbol{Q}}_k, \bar{\gamma})$, $\eta_\ell$ and $\omega_\ell$ are functions of large scale fading and given in Section VII-D. Employing (21) in (20), we obtain an approximation for the average error rate of user $k$:

$$\text{SER}_k \approx a \Theta_k \sum_{\ell=1}^{n_R} \frac{1}{\omega_{k\ell}} \left( 1 - \sqrt{\frac{2g}{2g + \omega_{k\ell}}} \right) \quad \forall\, k, \tag{22}$$

where $\Theta_k = \Delta_k(\bar{\boldsymbol{Q}}_k, \bar{\gamma}) |\boldsymbol{P}_k|^{-1} d_k^{-L}$. We next formulate the optimization problem which forms the heart of this contribution. The optimum power loading vector $\boldsymbol{d}^* = (d_1^*, \ldots d_N^*)$ is given by

$$\boldsymbol{d}^* = \arg\min f(\boldsymbol{d}), \tag{23a}$$

$$\text{SER}_k|_{\bar{\gamma}=\text{SNR}_0} \leq \bar{\alpha}_k, \quad \forall\, k, \tag{23b}$$

$$d_k > 0 \quad \forall\, k., \tag{23c}$$

$$f(\boldsymbol{d}) = \sum_{k=1}^{N} d_k. \tag{23d}$$

[1]The average bit error rate (BER) is a more fundamental performance measure than the average SER. It can also be expressed in Gaussian Q-function form for many modulation schemes. Therefore, the development here can be readily used with BER metrics.

In order to tackle this complex optimization problem, we consider a high SNR approximation for average SER originally reported in [11] for macrodiversity MU-MIMO systems. From Appendix A, the asymptotic SER for the $k$th user is given by

$$\text{SER}_k^{\infty} \simeq \frac{\mathcal{I}_k(\boldsymbol{P},\boldsymbol{D})\text{Perm}(\boldsymbol{Q}_k)}{|\boldsymbol{P}_k| d_k^L}\bar{\gamma}^{-L}, \quad \forall\, k, \tag{24}$$

where the integral $\mathcal{I}_k(\boldsymbol{P},\boldsymbol{D})$ is given by

$$\mathcal{I}_k(\boldsymbol{P},\boldsymbol{D}) = \frac{a}{\pi}\int_0^T \frac{\left(\prod_{u\neq k}^{N}\frac{d_u}{d_k}\right)\sin^{2n_R}\theta}{\sum_{i=0}^{N-1}\zeta_i g^{n_R-i}\sin^{2i}\theta}d\theta, \tag{25}$$

and $\bar{\gamma} = 1/\sigma^2$. It may be useful to point out here that the integral $\mathcal{I}_k(\boldsymbol{P},\boldsymbol{D})$ that appears in (25) depends on $\boldsymbol{D}$ only through ratios $d_u/d_k$ for $\forall\, u \neq k$. The integral in (25) can be solved in closed form but, in this work we are rather interested in its current form as it appears in (25). Even though the expression in (70) appears complicated, the final solution after simplifications is appealing as shown in (26), shown at the bottom of the page, for the first user for $N = 3$ where $\boldsymbol{R}_1 = \boldsymbol{P}_1^{-1}\boldsymbol{Q}_1$, and $\boldsymbol{R}_{11}$ and $\boldsymbol{R}_{12}$ are the first and second column of $\boldsymbol{R}_1$.

Using the high SNR affine approximation, we recast our original optimization problem equivalently by

$$\boldsymbol{d}^* = \arg\min f(\boldsymbol{d}), \tag{27a}$$

$$\text{SER}_k^{\infty}|_{\bar{\gamma}=\text{SNR}} \leq \alpha_k, \quad \forall k, \tag{27b}$$

$$d_k > 0 \quad \forall\, k., \tag{27c}$$

$$f(\boldsymbol{d}) = \sum_{k=1}^{N} d_k. \tag{27d}$$

Here we transform the original SER constraints to an equivalent high SNR SER constraints as explained in Section VII-D. The optimization problem in (27) can be solved using a simple algorithm. The algorithm runs through a series of iterations until power loading vector converges to a steady state. Let's define the power loading vector in the $l$th iteration as $\boldsymbol{d}_l = (d_{l,1}, \ldots d_{l,N})$. We start with an initial power loading vector, $\boldsymbol{d}_0$ in such a way that it has all equal elements (i.e., $d_{0,1} = \ldots = d_{0,N}$). The $k$th user's power level in the $(l+1)$th iteration is functionally related to the power level of all users in the system in the $l$th iteration (i.e., $\boldsymbol{d}_l$) and is given by

$$d_{l+1,k} = \left(\frac{\mathcal{I}_k(\boldsymbol{P},\boldsymbol{D})_l\text{Perm}(\boldsymbol{Q}_k)\text{SNR}^{-L}}{|\boldsymbol{P}_k|\alpha_k}\right)^{\frac{1}{L}}, \quad \forall\, k, \tag{28}$$

where

$$\mathcal{I}_k(\boldsymbol{P},\boldsymbol{D})_l = \mathcal{I}_k(\boldsymbol{P},\boldsymbol{D})|_{\boldsymbol{D}=\text{diag}(d_{l1},\ldots,d_{l,N})}. \tag{29}$$

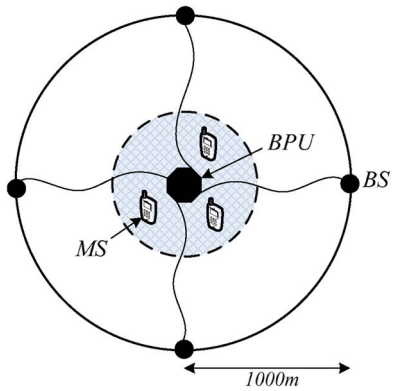


Fig. 1. A network MIMO system with four BSs forming a large macrocell.

In Section VII-A we will show that, the power loading vector obtained here is in fact the optimal solution which minimize the objective function while satisfying the SER constraints.

## VI. Numerical Results and Discussion

As numerical results, we confirm the accuracy of the power control algorithm by using a base line edge-excited network MIMO setting in Fig. 1 [11]. For each uniform random location of the users in the circular coverage area, log-normal shadow fading and path loss effects are considered where $\sigma_{SF} = 8$ dB (standard deviation of shadow fading) and the path loss exponent is 3.5. The BSs are located on the edge of the coverage area with 90° angular separation. There is a 35 m user exclusion zone around BSs. Since, cell coordination has a profound effect on cell-edge users, we only consider user drops inside the circular shaded region of 500 m radius which represents the cell edge of all BSs. This setting allows us to generate a wide range of $\boldsymbol{P}$ matrices[2] with entries which mimic those encountered in systems experiencing slow fading. Then, the channel matrix, $\boldsymbol{H}$ is simulated as

$$\boldsymbol{H} = \left(\boldsymbol{P}^{\circ\frac{1}{2}}\right) \circ \boldsymbol{U}, \tag{30}$$

where $\boldsymbol{P}^{\circ(1/2)}$ is the element-wise square root of $\boldsymbol{P}$, the operator, $\circ$, represents Hadamard multiplication and the elements, $\boldsymbol{U}_{ik}$, of $\boldsymbol{U}$ satisfy $\boldsymbol{U}_{ik} \sim \mathcal{CN}(0,1)\ \forall\, i,k$. The matrix $\boldsymbol{U}$ represents the Rayleigh distributed fast fading effect while $\boldsymbol{P}$ captures the large-scale fading effect. The fast fading, $\boldsymbol{U}$ is assumed to be changing every channel use while $\boldsymbol{P}$ remains constant for several channel use. Therefore, those power control methods adapt to CSI (i.e., $\boldsymbol{H}$), have to be updated every channel use while power control methods adapt to CDI needed to be updated only when $\boldsymbol{P}$ changes.

[2]It may be useful to note here that, we employ $P_{ik} = 99.54 - 35\log_{10} d + \Psi_{ik}$ [dB] which is the decibel version of (5) for generating macrodiversity power profiles.

$$\text{SER}_1^{\infty} \simeq \frac{a}{\pi}\int_0^T \frac{\bar{\gamma}^{-L} d_2 d_3 \text{Perm}(\boldsymbol{Q}_1)\sin^{2n_R}\theta}{|\boldsymbol{P}_1| d_1^{n_R}\left(g^{n_R} + \left(\frac{d_2}{d_1}\text{Perm}(\boldsymbol{R}_{11}) + \frac{d_3}{d_1}\text{Perm}(\boldsymbol{R}_{12})\right)g^{n_R-1}\sin^2\theta + \left(\frac{d_2 d_3}{d_1^2}\right)\text{Perm}(\boldsymbol{R}_1)g^{n_R-2}\sin^4\theta\right)}d\theta \tag{26}$$

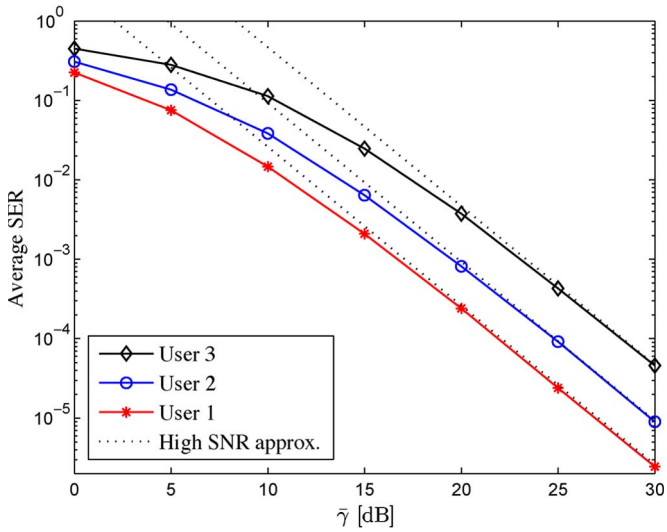


Fig. 2. Average SER vs $\bar{\gamma}$ for all three users with MMSE receive combining and QPSK constellation with equal transmit power levels. All power levels are set to 0 dB.

The Fig. 2 shows the uncoded average SER of all three users with MMSE receive combining and QPSK constellation for a typical macrodiversity power profile. The high SNR approximations in (24) are also shown for comparison and equal power transmission[3] is considered (i.e., $d_1 = d_2 = d_3 = 1$). According to Fig. 2, it is clear that three users exhibit SER performance differences in terms of array gain. We assume there is a design goal such that at SNR $= 25$ dB, we have to make sure that all users have SER of $10^{-4}$. In order to achieve this goal we apply the algorithm in (28) with initial power loading vector, $\boldsymbol{d}_0 = (1/3, 1/3, 1/3)$. After about 7 iterations, we arrive at a steady state power loading vector and is given by

$$\boldsymbol{d}_7 = (0.6118,\ 0.9929,\ 1.9808). \tag{31}$$

We conclude that $\boldsymbol{d}_7$ is indeed the optimal power vector, $\boldsymbol{d}^*$ for this particular $\boldsymbol{P}$, SNR and SER thresholds. In order to understand this result, lets consider the macrodiversity power profile matrix, $\boldsymbol{P}$ used in this simulation:

$$\boldsymbol{P} = \begin{pmatrix} 0.5886 & 0.2326 & 0.2028 \\ 0.4443 & 0.0734 & 0.1854 \\ 0.7819 & 0.3135 & 0.1294 \\ 0.2349 & 0.7672 & 0.1107 \end{pmatrix}. \tag{32}$$

This $\boldsymbol{P}$ corresponds to a macrodiversity system with $n_R = 4$ distributed BS antennas and $N = 3$ distributed users. The sum receive (RX) power (i.e., $\sum_i P_{ik}$ for $\forall\, k$) of all three users are given in Table I. If we compare the transmit power differences of user 1 and 3, it is not surprising that user 3 needs to transmit at higher power to achieve the same SER target while user 1 needs much less than that due to its favorable large scale fading gains which is noticeable in the sum RX power in Table I. Even though such comparisons are possible with primitive metrics like sum RX power, we need results presented in Section V-B to make concrete conclusions.

[3]Unless otherwise stated, all power values are given in linear scale.

TABLE I
SUMMARY OF RESULTS FOR S1

| User | Sum RX power | TX power | SER, SNR [dB] |
|---|---|---|---|
| 1 | 2.0497 | 0.6118 | $10^{-4}$, 25 |
| 2 | 1.3867 | 0.9929 | $10^{-4}$, 25 |
| 3 | 0.6283 | 1.9808 | $10^{-4}$, 25 |

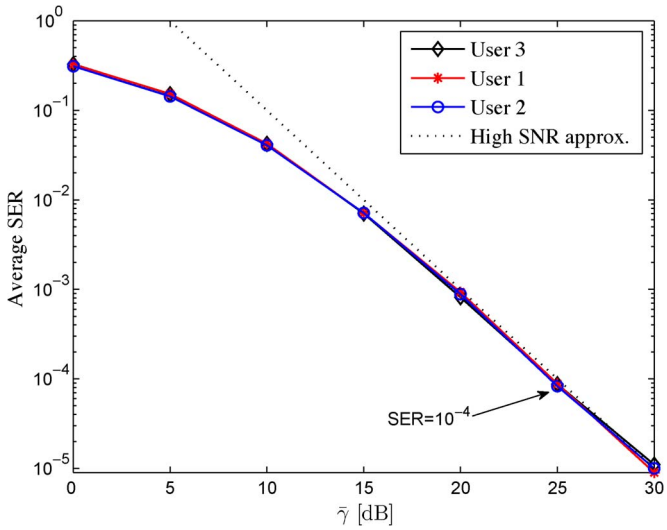


Fig. 3. Average SER vs $\bar{\gamma}$ for all three users with MMSE receive combining and QPSK constellation after applying power control algorithm.

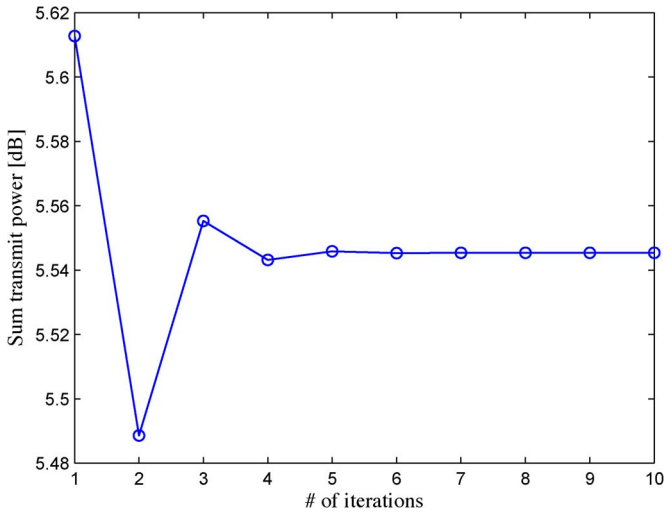


Fig. 4. Sum transmit power variation against the number of iterations in scenario 1 for specifications in Table I.

Fig. 3 shows the SER curves after applying the optimum power loading vectors. It is clearly visible that the SER performance is very much comparable and error rates of $10^{-4}$ at SNR $= 25$ dB are clearly achieved. The slight difference in the SER performance is due to the approximation in (64).

Next, we consider the rate of convergence of the main algorithm. In Fig. 4, the sum transmit power distribution against the number of iterations is shown. It can be seen that there is an oscillation until $l = 6$ but the magnitude of the oscillation appears to be decaying very rapidly allowing the power vector to be stable at the 7th iteration. Therefore, it is clear that the rate of convergence is quite reasonable for many practical applications.

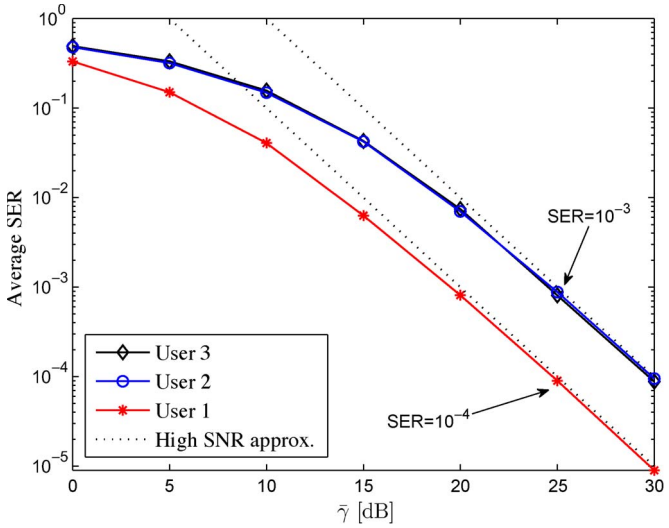


Fig. 5. Average SER vs $\bar{\gamma}$ for all three users with MMSE receive combining and QPSK constellation after applying revised transmit power levels to satisfy unequal SER targets.

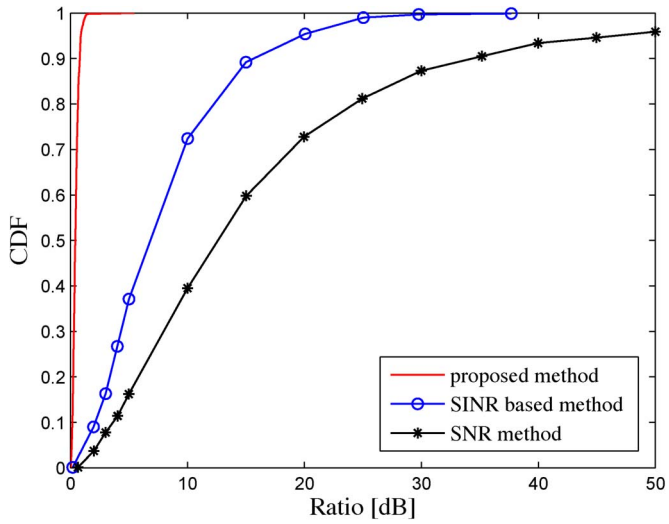


Fig. 6. Comparison of the average SER performance of the proposed algorithm against exiting SNR and SINR based algorithms.

Next we consider an extended version of the simulation scenario so far where we set unequal error rate targets for each user in the system. This is a practical problem due to the fact that voice and data users may have different QoS constraints, but may well be scheduled in the same transmission interval. Therefore, we set $\text{SER}_1^{\infty} = 10^{-4}$ and $\text{SER}_2^{\infty} = \text{SER}_3^{\infty} = 10^{-3}$ at $\bar{\gamma} = 25$ dB. The results are shown in Fig. 5 and performance exhibits an acceptable match with specifications.

We next simulate large number of large-scale fading profiles (thus, $\boldsymbol{H}$) and study several important metrics. We observe that our algorithm converges in all realizations of macrodiversity power profiles. It is calculated that the average number of iterations for convergence is about 6 for average SER of $10^{-4}$ at 25 dB. It is further observed that the more square the system (i.e., $n_R \approx N$) the higher the average number of iterations, and the average number of iterations drops rapidly for rectangle systems (i.e., $n_R > N$), which is the case in many modern MU-MIMO systems. For instance, when each BS has two co-located antennas which gives $n_R = 8$ and $N = 3$ the algorithm converges within about three iterations. Furthermore, zero-forcing (ZF) based direct method expends about 10% more total transmit power than MMSE based method. It may be worthwhile to note here that ZF based method has an additional drawback due to its relatively weaker SER approximation so that it may not follow actual SER as accurate as MMSE based method.

In Fig. 6, the accuracy of the proposed SER based method is compared with existing SINR based methods. We assume the same cellular setting as shown in the Fig. 1 with dual antenna BSs. Therefore, it gives $n_R = 8$. We further assume there are $N = 3$ co-scheduled users in the coverage area. Our experiment runs as follows. We simulate a large number of $8 \times 3$ macrodiversity power profiles. For each $\boldsymbol{P}$ matrix, we calculate the optimal transmit power levels for all users to achieve a SER target of $10^{-2}$ at $\bar{\gamma} = 5$ dB with QPSK modulation. Then we obtain the SERs of all users at $\bar{\gamma} = 5$ dB with the same $\boldsymbol{P}$ matrix and its corresponding power loading vector using Monte Carlo simulation. We define the vector, $\text{SER}_s = (\text{SER}_{s1}, \text{SER}_{s2}, \text{SER}_{s3})$. Similarly, SNR and SINR metrics are computed for all three users using (16) and (18). Then we translate these SNR and SINR metrics into an error probability value using the following SER result for QPSK modulations [12]:

$$\text{SER}(x) = 1 - \left(1 - Q(\sqrt{x})\right)^2, \tag{33}$$

where $x$ is the SNR or SINR as defined in (16) and (18). From (33), we calculate corresponding SER values for SNR metrics, denoted $\text{SER}_a = (\text{SER}_{a1}, \text{SER}_{a2}, \text{SER}_{a3})$ and for SINR metrics, denoted $\text{SER}_b = (\text{SER}_{b1}, \text{SER}_{b2}, \text{SER}_{b3})$. The subscripts $a$ and $b$ are used to distinguish the variable and have no further significance on the result of the paper. Then we compute the ratio between the lowest and the highest error rates in all three methods. Let the ratio obtained from simulation is denoted by, $r_s$:

$$r_s = \frac{\max(\text{SER}_s)}{\min(\text{SER}_s)}. \tag{34}$$

Similarly, we define $r_a$ and $r_b$ to denote the ratios obtained from SNR and SINR based methods respectively. If the proposed method is accurate, the $r_s$ should be equal to unity. Furthermore, if SNR and SINR based methods capture the performance of users accurately, $r_a$ and $r_b$ also should be equal to $r_s$. The cumulative distribution function of the average SER ratio is given in Fig. 6 for all three methods. We observe that the proposed method is extremely accurate than conventional methods. Its CDF is almost a straight line with a subtle shift. This small shift is due to the original approximation used for SERs in (22). The considerable gap between the CDF curves of $r_b$ and $r_s$ clearly proves that SINR based method is extremely poor at capturing the performance of users. It is worse in $r_a$ case. The SER ratio, $r_b$ is greater than 3 dB in 80% of the time. It is clear from $r_s$ curve that all users have approximately comparable error performance. However, from the CDF curve for $r_b$, the SINR based metric can misinterpret it as a SER

performance gap of 5 dB or more between the best and the worst user in 60% of the time. It can be higher than 10 dB in 25% of the time. Therefore, those power controlling methods which adjust the SINR metric to be equal end up altering already comparable SER performance considerably. In addition, power control algorithms based on these SNR/SINR metrics can be energy inefficient as a result of their lower sensitivity to performance of users. This result however, does not surprise us owing to the fact that proposed power control solution is based on a metric which has a direct functional link to error performance of users while other methods broadly rely on *ad-hoc* metrics of which the relationship to error performance is not clear.

## VII. Further Remarks

### A. Optimality of the Main Algorithm

From an optimization-theoretic point of view, the optimization problem in (23) poses some theoretical challenges on which we devote this section. Assume the candidate optimal solution is $\boldsymbol{d}^*$. Let's define the Lagrange function as

$$L(\boldsymbol{d}) = -f(\boldsymbol{d}) + \sum_{k=1}^{N} \lambda_k \left(\alpha_k - \mathrm{SER}_k^{\infty}(\boldsymbol{d})\right), \tag{35}$$

where $\lambda_k$ are Lagrange multipliers. Karush-Kuhn-Tucker (KKT) conditions at the optimal point can be derived as [27]

$$-\nabla f(\boldsymbol{d}^*) - \sum_{k=1}^{N} \lambda_k \nabla \mathrm{SER}_k^{\infty}(\boldsymbol{d}^*) = 0, \tag{36}$$

$$\alpha_k - \mathrm{SER}_k^{\infty}(\boldsymbol{d}^*) \geq 0, \ \forall\, k, \tag{37}$$

$$\lambda_k \geq 0, \ \forall\, k, \tag{38}$$

$$\lambda_k \left(\alpha_k - \mathrm{SER}_k^{\infty}(\boldsymbol{d}^*)\right) = 0, \ \forall\, k, \tag{39}$$

where $\nabla L(\boldsymbol{d}^*)$ is the derivative of $L(\boldsymbol{d})$ with respect to $\boldsymbol{d}$ evaluated at $\boldsymbol{d} = \boldsymbol{d}^*$. The condition in (36) is due to the positivity constraint of $\boldsymbol{d}$. Furthermore, due to the fact that $f(\boldsymbol{d})$ has no critical points, the optimal point should lie on the boundary of the feasible set. It implies that, $\alpha_k - \mathrm{SER}_k^{\infty}(\boldsymbol{d}^*) = 0$ and $\lambda_k > 0$. Since, all $\nabla \mathrm{SER}_k^{\infty}(\boldsymbol{d}^*)$ are linearly independent, we further claim that all $\lambda_k$ should be strictly positive at the optimal point simultaneously.[4] This confirms that, from (39) all original inequality constraints should be simultaneously satisfied with equality constraints at the optimal $\boldsymbol{d}^*$. Therefore, ultimately the optimization problem boils down to solving non-linear simultaneous equations due to the fact that there are as many constraints as unknowns. The algorithm in (28) effectively does that by making sure that iterative process will converge to a fix power loading vector. We avoid negative power levels by neglecting the negative roots in (28). However, it is not sufficient to warrant that it is the optimal solution due to the uncertainty of the convexity of the feasible set. Since, it is the only vector with all positive power levels which satisfy the KKT conditions, we can assure that it is indeed the optimal solution. In order to check our assertions, we perform a simulation study with an arbitrary macrodiversity power profile given by

$$\boldsymbol{P} = \begin{pmatrix} 0.6160 & 0.3517 \\ 0.4733 & 0.8308 \end{pmatrix}. \tag{40}$$

We use $N = 2$ scenario here because it allows us to present results graphically. The algorithm gives $\boldsymbol{d}^* = (3.8102,\ 3.5981)$ as the optimal solution to satisfy SER targets of $10^{-3}$ at SNR $=$ 25 dB. In Fig. 7, we show the feasible set for the power profile in (40) and specifications considered in this section. Apparently, the feasible set is not convex. Among infinite number of candidate optimal vectors on the boundary of red region, the solution given by the algorithm in (28) is shown in black spot at the bottom of the feasible region. Therefore, it clearly, minimizes the sum transmit power.

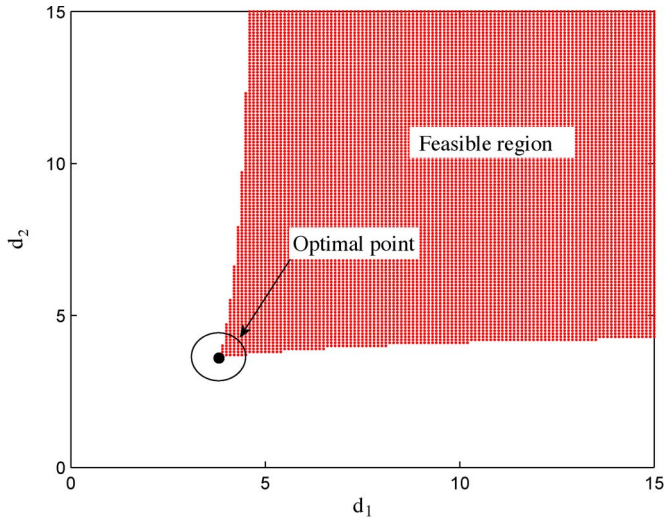


Fig. 7. Feasible set and optimal point for the macrodiversity power profile in (40).

### B. Feasibility of SER Constraints

Since, there are no upper and lower limits except strict positivity for the transmit powers, $d_k$ for $\forall\, k$, theoretically any SER target can be achieved. However, many practical scenarios, there are upper limits for transmit powers as given by

$$0 < d_k \leq U_k, \ \forall\, k. \tag{41a}$$

Note that in many scenarios it is reasonable to assume $U_1 = U_2 = \cdots = U_N = U$. We assume that a scheduling decision has been made to serve all $N$ users in the system. This implies that $d_k \neq 0$. Alternatively, there may be fixed lower limits for transmit power such as $L_k \leq d_k$ for $\forall\, k$. Therefore, there exists a reasonable question that how we can set feasible SER targets in compliance with transmit power limits. With the presence of such lower and upper limits, we need to analyze the feasibility of SER targets before applying the algorithm. In order to achieve this target, we use the following pragmatic approach.

1) First we find the $k$th user's SER dynamic range. This can be accomplished by setting desired user's power level to its maximum and minimum and rest of the users' (interfering users') power levels to their minimums and

[4] In contrast to SINR based power control problems, proving linear independence analytically for general user case, appears complicated. However, authors proved it analytically for $n_R = N = 2$ system where $\mathrm{SER}^{\infty}$ are reduced to simpler expressions (see Appendix B).

maximums for finding the lowest and highest SER for user $k$ using the equation in (22). This is repeated for all $N$ users. Theoretically, any SER constraint set within these limits is feasible.

2) Next, according to the error rate requirements for the system, we set SER targets within above limits.
3) Finally, we can apply the main algorithm for finding the set of power levels which guarantee these performance limits with minimal sum transmit power.

### C. Simplified Power Control Solution

The power control solution presented in (28) is algorithmic and therefore, there may be interest for a simple one-off method where a reasonable solution could be found. There exists such a solution at the expense of accuracy. In [11], authors derives a high SNR approximation for the average SER with ZF receivers. It has been shown in [11] that the error performance of the $k$th user after ZF combining is

$$\mathrm{SER}_k^{\infty} = \frac{a}{\pi}\int_0^T \tilde{K}_0 \left(\frac{\sigma^2 \sin^2\theta}{g}\right)^L d\theta, \tag{42}$$

where

$$\tilde{K}_0 = \mathcal{E}\left\{\frac{\left|\tilde{\boldsymbol{H}}_k^H \tilde{\boldsymbol{H}}_k\right|}{|\tilde{\boldsymbol{P}}_k|\left|\tilde{\boldsymbol{H}}_k^H \tilde{\boldsymbol{P}}_k^{-1} \tilde{\boldsymbol{H}}_k\right|}\right\}. \tag{43}$$

After making the substitution in (63), we arrive at

$$\mathrm{SER}_k^{\infty} \simeq \frac{\mathrm{Perm}(\boldsymbol{Q}_k)\tilde{\mathcal{I}}}{|\boldsymbol{P}_k|\mathrm{Perm}\left(\boldsymbol{P}_k^{-1}\boldsymbol{Q}_k\right) d_k^L}\bar{\gamma}^{-L}, \quad \forall\, k, \tag{44}$$

where

$$\tilde{\mathcal{I}} = \frac{a}{\pi}\int_0^T \left(\frac{\sin^2\theta}{g}\right)^L d\theta. \tag{45}$$

From equation (44), it is clear that the SER of user $k$ depends on $\boldsymbol{D}$ through its own transmit power, $d_k$. Therefore, the transmit power of all users can be adjusted according to their SER targets, $\alpha_k$ independently. This avoids the algorithm in Section V-B.

The SER approximation in (44) and the main MMSE based approximation are tight when $n_R \gg N$. This constraint can easily be satisfied when coordinated BSs have multiple co-located antennas. In such scenarios, both approximations tend to be extremely tight. Furthermore, in Section VII-E, it has been shown that computational complexity, especially for permanent calculations (see Section IV) does not grow with the number of co-located antennas at each BS.

### D. Higher SER Targets at Low SNR

There may be some interests in having higher SER targets at low SNR. The proposed power control algorithm is based on a high SNR approximation in (24). It may not follow the average

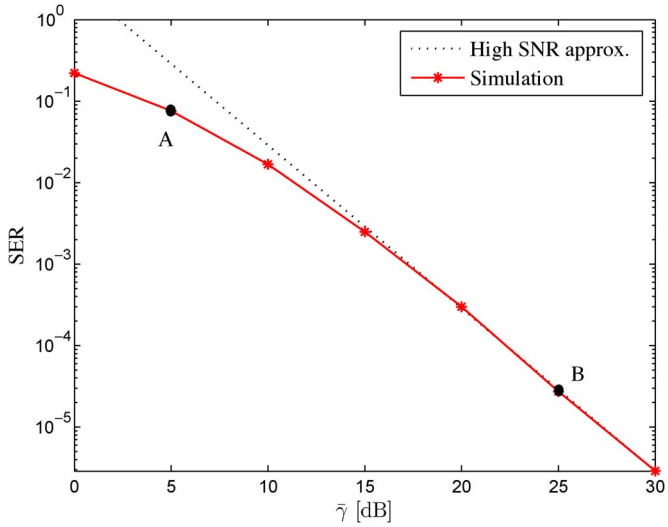


Fig. 8. Illustration of change of SER constraints of a typical user.

SER curves at higher error rates especially when $n_R > N$ case (see Fig. 2). This can be circumvented by using a method called '*change of constraints*' as depicted in Fig. 8. Since SER is a continuous function of SNR, every low SNR SER target has a high SNR counterpart. Assume we have an original SER constraint at $(\mathrm{SER}_k, \bar{\gamma}) = (\bar{\alpha}_k, \mathrm{SNR}_0)$ as shown from the point A in the Fig. 8. Clearly, $\mathrm{SER}_k^{\infty}$ does not capture the error performance. If an SER constraint at high SNR could be found in such a way that, one achieves the target SER at low SNR automatically if the high SNR target SER is achieved, the main algorithm can be used with the new high SNR constraint. The high SNR region in the sense that $\mathrm{SER}_k$ in (22) is equal to the $\mathrm{SER}_k^{\infty}$ in (24). One such point is shown by the point B in the same illustration. Therefore, if SER constraint can be represented by an equivalent $\mathrm{SER}^{\infty}$ constraint, the main algorithm in (28) can be applied readily. In cases where it is not possible to translate the low SNR target to a high SNR counterpart, we have to solve the original optimization problem in (23) should be solved. The average $\mathrm{SER}_k$ in (22) can also be given alternatively by

$$\mathrm{SER}_k \approx \frac{\mathcal{J}_k(\bar{\boldsymbol{P}}, \bar{\gamma})\Delta_k(\bar{\boldsymbol{Q}}_k, \bar{\gamma})}{|\boldsymbol{P}_k| d_k^L}, \tag{46}$$

where

$$\mathcal{J}_k(\bar{\boldsymbol{P}}, \bar{\gamma}) = \frac{a}{\pi}\sum_{i=1}^{n_R}\int_0^T \frac{\eta_i \sin^2\theta}{g + \omega_i \sin^2\theta} d\theta. \tag{47}$$

The coefficients $\omega_i$s in the denominator of (47) are given by the roots of the following polynomial:

$$\sum_{i=1}^{n_R} \varphi_i x^i = 0, \tag{48}$$

where, $\varphi_i$ is given by [11, eq. 60],

$$\varphi_i = \sum_{k=1}^{N-1} \hat{\varphi}_{ik} \bar{\gamma}^{i-k-N+1} \tag{49}$$

and, $\hat{\varphi}_{ik}$ in (49) is given by

$$\hat{\varphi}_{ik} = d_k^i \sum_{\sigma} \mathrm{Tr}_i \left( (\boldsymbol{P}_k)_{\bar{\sigma}_{n_R-k,n_R}} \right) \mathrm{Perm} \left( (\bar{\boldsymbol{Q}}_k)_{\sigma_{k,n_R}}^{\{N-1\}} \right). \tag{50}$$

The $\sigma_{k,n_R}$ is an ordered subset of $\{n_R\} = \{1, \ldots, n_R\}$ of length $k$ and the summation is over all such subsets. The $\bar{\sigma}_{n_R-k,n_R}$ is a length $n_R - k$ subset of $\{1, \ldots, n_R\}$ which does not belong to $\sigma_{k,n_R}$. Furthermore, $\eta_i$ in (47) is given by

$$\eta_i = \frac{1}{\prod_{\ell \neq i}^{n_R} (\omega_\ell - \omega_i)}. \tag{51}$$

The $\Delta_k(\bar{\boldsymbol{Q}}_k, \bar{\gamma})$ in (46) is given by

$$\Delta_k(\bar{\boldsymbol{Q}}_k, \bar{\gamma}) = d_k^{-N+1} \sum_{k=0}^{N-1} \sum_{\sigma} \mathrm{Perm} \left( (\bar{\boldsymbol{Q}}_k)^{\sigma_{k,N-1}} \right) \bar{\gamma}^{-N+k+1}. \tag{52}$$

Note that the matrices $\bar{\boldsymbol{P}} = \boldsymbol{P}\boldsymbol{D}$ and $\bar{\boldsymbol{Q}}_k = \boldsymbol{Q}_k \boldsymbol{D}_k$. The $\mathrm{SER}_k$ approximation in (46) is in fact the parent approximation for SER from which $\mathrm{SER}_k^{\infty}$ is derived by discarding the lower order negative powers of $\bar{\gamma}$. The added complexity of $\mathrm{SER}_k$ is clearly understandable because, the lower order negative powers of $\bar{\gamma}$ can not be neglected if the approximation needs to follow the actual average SER at low SNR. Similar to the original algorithm, the power level of the $k$th user in the $(l+1)$th iteration is functionally related to the power level of all users in the system in the $l$th iteration (i.e., $\boldsymbol{d}_l$) and is given by

$$d_{l+1,k} = \left( \frac{\mathcal{J}_k(\bar{\boldsymbol{P}}, \bar{\gamma})_l \Delta_k(\bar{\boldsymbol{Q}}_k, \bar{\gamma})}{|\boldsymbol{P}_k| \bar{\alpha}_k} \right)^{\frac{1}{L}}, \quad \forall\, k, \tag{53}$$

where

$$\mathcal{J}_k(\bar{\boldsymbol{P}}, \bar{\gamma})_l = \mathcal{J}_k(\bar{\boldsymbol{P}}, \bar{\gamma})\big|_{\boldsymbol{D}=\mathrm{diag}(d_{l1},\ldots,d_{l,N})}. \tag{54}$$

This algorithm is used extensively in generating Fig. 6 where a system is optimized to achieve a higher SER targets at very low SNR.

### *E. Computational Complexity of the Main Algorithm*

In this section, we present a complexity analysis for the main algorithm in (28) is presented. For that, we consider square systems (i.e., $n_R = N$) with varying dimensions, $N = 2$, 3, 4, 5. This is corresponding to $N$ number of single receive antenna distributed BSs and single antenna users. Therefore, it creates a macrodiversity power profile matrix with no duplicate columns and rows. The evaluation of the integration in (25) is computationally demanding. We may use two methods to evaluate it. In the first method, the denominator is assumed as a polynomial of $\sin^2\theta$ thus, can be expressed as a product of $N-1$ terms. Using the partial fraction expansion method, the integration can be expressed as shown in (47) where individual integrations can be solved in closed form. The roots of the polynomial can be found by evaluating the eigenvalues of the corresponding $\mathcal{R}^{(N-1)\times(N-1)}$ companion matrix [28]. We assume here that the calculation of coefficients, $\zeta_i$s and roots of the denominator polynomial are computationally significant.

TABLE II
COMPUTATIONAL COMPLEXITY OF THE MAIN ALGORITHM IN (28)

| N | # of multiplications |
|---|---|
| 2 | 204 |
| 3 | 1188 |
| 4 | 5952 |
| 5 | 49650 |

Furthermore, the average number of iteration is taken to be 6. The results are shown in Table II. In the second method, it is assumed that the integration is evaluated directly using Trapezoidal rule with $n = 24$ subintervals for the integration over $[0, T]$ [29]. The integrand in (25) should be evaluated $n-1$ times to calculate the integration over the desired region. It therefore, may be computationally inefficient in comparison with the first method, and results are omitted.

With the advent of massive MIMO concepts, there may be practical interests of BSs with large number of co-located receive antennas [30]. In that cases, macrodiversity power profile matrix has duplicate entries which can be exploited for simplifying permanent calculations as follows. Consider a scenario where a BS has co-located $W$ receive antennas. We explain this with a simple example, but extensions are straightforward. Let the $3 \times 3$ matrix $\boldsymbol{P}$ be,

$$\boldsymbol{P}|_{W=1} = \begin{pmatrix} a & b & c \\ d & e & f \\ g & h & i \end{pmatrix}. \tag{55}$$

This corresponds to a system with three users and 3 BS with a single antenna each, i.e., $W = 1$. If each BS has $\mu$ receive antennas, the $3\mu \times 3$ matrix $\boldsymbol{P}$ becomes

$$\boldsymbol{P}|_{W=\mu} = \begin{pmatrix} a & b & c \\ \cdots & \cdots & \cdots \\ a & b & c \\ d & e & f \\ \cdots & \cdots & \cdots \\ d & e & f \\ g & h & i \\ \cdots & \cdots & \cdots \\ g & h & i \end{pmatrix}. \tag{56}$$

Assume $\mu \geq 3$. The $\mathrm{perm}(\boldsymbol{P}_{W=\mu})$ is given in (57), shown at the bottom of the next page. The expression in (57) is obtained by applying the following permanent identity, and with some simplifications. Let $\boldsymbol{A}$ be an arbitrary $m \times n$ matrix and assume $m \geq n$, then

$$\mathrm{Perm}(\boldsymbol{A}) = \sum_{\sigma} \mathrm{perm} \left( (\boldsymbol{A})_{\sigma_{n,m}} \right) \tag{58}$$

where $\sigma_{n,m}$ is an ordered subset of $\{m\} = \{1, \ldots, m\}$ of length $n$ and the summation is over all such subsets. $\boldsymbol{A}_{\sigma_{n,m}}$ denotes the submatrix of $\boldsymbol{A}$ formed by taking only rows indexed by $\sigma_{n,m}$ and all columns. Note that the constituent permanents with duplicate rows in (57) have further simplifications. Apart from the apparent fact that the computational complexity of (57) is much lower than direct calculation of $\mathrm{perm}(\boldsymbol{P}|_{W=\mu})$ using (58), it is also clear that the computational complexity does not grow with $\mu$. Therefore, the practical implications of

this example to our system is that the computational cost grows with the number of users and BSs, but not with the co-located antennas at each BS.

### F. Convergence of the Main Algorithm

It is shown in Section VII-A that the main optimization problem reduces to a system of $N$ non-linear equations. One common method of solving such a system is to use Newton-Raphson method where a Jacobian matrix has to be evaluated in every iteration [31]. In such cases, the convergence is always not guaranteed and depends on several factors specially the initial estimate. Due to the unique structure of $\mathcal{I}_k(\boldsymbol{P}, \boldsymbol{D})$, we avoid the initial value problem where algorithm itself positions on the right path after the first iteration. It is because $\mathcal{I}_k(\boldsymbol{P}, \boldsymbol{D})$ depends on $\boldsymbol{d}$ not through their absolute values but ratios. Therefore, if initial estimates of all transmit powers are set to the same level, we *may* avoid oscillating the algorithm. However, it is not sufficient to warrant the convergence of the algorithm. A rigorous proof is left to a future work. Furthermore, our simulation study shows that convergence is always attainable in the typical cellular model considered in the paper.

## VIII. Conclusion

In this paper we considered a power control problem for MU CoMP systems with JP. Primarily, it targets at overcoming large-scale fading, and hence based on CDI. In contrast to the existing power control methods which are based on crude performance metrics, we present a systematic power control algorithm in order to minimize the transmit power while achieving certain QoS constraints by exploiting recently published analytical performance results for average error rates. Our QoS metric was the average SER after MMSE receive combining rather than conventional SNR/SINR based metrics before any receive processing. Despite the analytical complexity of this particular problem, we are able to come to a tractable conclusion proposing an optimal power control algorithm which minimizes the sum transmit power while guaranteeing given SER targets at a given SNR. Simulation results show that SER curves follow the predicted performance accurately proving the accuracy of the power control method. Furthermore, we proved the optimality of the proposed power control algorithm even though the feasible set is not convex. Before concluding our paper, we further commented on finding feasible SER constraints along with a simplified power control method based on ZF receive combining for applications where accuracy could be traded off for simplicity. Even though the proposed power control solution is slightly more complex than existing solutions, our results show that it is well worth adopting to modern multi-cell communication systems as far as its superior performance and accuracy are considered. We hope these tools will help system engineers to design wireless systems with network coordination with a much greater grip and minimal power consumption.

## Appendix A
## Derivation of Asymptotic SER

The local average SER of the $k$th user for $M$-PSK and $M$-QAM type modulation schemes can also be evaluated as [12]

$$\mathrm{SER}_k = \frac{a}{\pi}\int_0^T \mathcal{M}_{Z_k}\left(-\frac{g}{\sin^2\theta}\right)d\theta, \quad \forall\, k, \tag{59}$$

where $\mathcal{M}_{Z_k}(.)$ is the moment generating function of the $k$th user's SINR after receive combining. From [11], the SER when $\sigma^2 \to 0$ becomes

$$\mathrm{SER}_k^{\infty} = \frac{a}{\pi}\int_0^T \left(\frac{\sigma^2\sin^2\theta}{g}\right)^L K_0\left(\frac{g}{\sin^2\theta}\right)d\theta \tag{60}$$

where $L = n_R - N + 1$ and

$$K_0(s) = \mathcal{E}\left\{\frac{\left|\tilde{\boldsymbol{H}}_k^H\tilde{\boldsymbol{H}}_k\right|}{|\tilde{\boldsymbol{P}}_k|\left|\tilde{\boldsymbol{H}}_k^H\tilde{\boldsymbol{P}}_k^{-1}\tilde{\boldsymbol{H}}_k + s\boldsymbol{I}\right|}\right\}. \tag{61}$$

The matrices appearing in (61) are defined as follows.

$$\tilde{\boldsymbol{H}}_k = \boldsymbol{H}_k\boldsymbol{D}_k, \tag{62}$$

$$\tilde{\boldsymbol{P}}_k = d_k\boldsymbol{P}_k, \tag{63}$$

$$\begin{aligned}\mathrm{Perm}(\boldsymbol{P}|_{W=\mu}) = {} & \binom{\mu}{1}\binom{\mu}{1}\binom{\mu}{1}\mathrm{perm}\begin{pmatrix}a&b&c\\d&e&f\\g&h&i\end{pmatrix} + \binom{\mu}{2}\binom{\mu}{1}\\ & \times\left(\mathrm{perm}\begin{pmatrix}a&b&c\\a&b&c\\d&e&f\end{pmatrix} + \mathrm{perm}\begin{pmatrix}a&b&c\\a&b&c\\g&h&i\end{pmatrix} + \mathrm{perm}\begin{pmatrix}d&e&f\\d&e&f\\g&h&i\end{pmatrix}\right.\\ & \left. + \mathrm{perm}\begin{pmatrix}d&e&f\\d&e&f\\a&b&c\end{pmatrix} + \mathrm{perm}\begin{pmatrix}a&b&c\\g&h&i\\g&h&i\end{pmatrix} + \mathrm{perm}\begin{pmatrix}d&e&f\\g&h&i\\g&h&i\end{pmatrix}\right)\\ & + \binom{\mu}{3}\left(\mathrm{perm}\begin{pmatrix}a&b&c\\a&b&c\\a&b&c\end{pmatrix} + \mathrm{perm}\begin{pmatrix}d&e&f\\d&e&f\\d&e&f\end{pmatrix} + \mathrm{perm}\begin{pmatrix}g&h&i\\g&h&i\\g&h&i\end{pmatrix}\right)\end{aligned} \tag{57}$$

where $\boldsymbol{H}_k$ is $\boldsymbol{H}$ with column $k$ removed, $\boldsymbol{D}_k$ is $\boldsymbol{D}$ with $k$th element removed, and the diagonal matrix $\boldsymbol{P}_k = \mathrm{diag}(P_{1,k}, P_{2,k}, \ldots, P_{n_R k})$. $K_0$ can be approximated by

$$K_0(s) \simeq \frac{\mathcal{E}\left\{\left|\tilde{\boldsymbol{H}}_k^H \tilde{\boldsymbol{H}}_k\right|\right\}}{\mathcal{E}\left\{|\tilde{\boldsymbol{P}}_k|\left|\tilde{\boldsymbol{H}}_k^H \tilde{\boldsymbol{P}}_k^{-1} \tilde{\boldsymbol{H}}_k + s\boldsymbol{I}\right|\right\}}. \tag{64}$$

The approximation has been shown to be tight for macrodiversity power profile $\boldsymbol{P}$ in cellular wireless systems [11, Section VII]. The expectations in both numerator and denominator of (64) can be evaluated in closed form, and are given by

$$\mathcal{E}\left\{\left|\tilde{\boldsymbol{H}}_k^H \tilde{\boldsymbol{H}}_k\right|\right\} = \mathrm{Perm}(\boldsymbol{Q}_k \boldsymbol{D}_k), \tag{65}$$

$$= \left(\prod_{u\neq k}^{N} d_u\right) \mathrm{Perm}(\boldsymbol{Q}_k), \tag{66}$$

where $\boldsymbol{Q}_k$ is $\boldsymbol{P}$ with column $k$ removed and

$$\mathcal{E}\left\{|\tilde{\boldsymbol{P}}_k|\left|\tilde{\boldsymbol{H}}_k^H \tilde{\boldsymbol{P}}_k^{-1} \tilde{\boldsymbol{H}}_k + s\boldsymbol{I}\right|\right\} = d_k^{n_R}|\boldsymbol{P}_k|\left(\sum_{i=0}^{N-1} \zeta_i s^{N-i-1}\right), \tag{67}$$

where

$$\zeta_i = \sum_{\sigma} \mathrm{Perm}\left(\left(\tilde{\boldsymbol{P}}_k^{-1}\boldsymbol{Q}_k\boldsymbol{D}_k\right)^{\sigma_{i,N-1}}\right), \tag{68}$$

$$= \sum_{\sigma} \frac{\left|(\boldsymbol{D}_k)_{\sigma_{i,N-1}}\right|}{d_k^i} \mathrm{Perm}\left(\left(\boldsymbol{P}_k^{-1}\boldsymbol{Q}_k\right)^{\sigma_{i,N-1}}\right), \tag{69}$$

where $\sigma_{i,N-1}$ is an ordered subset of $\{N-1\} = \{1, \ldots, N-1\}$ of length $i$ and the summation is over all such subsets. Note that $\zeta_0 = 1$ and

$$\zeta_{N-1} = \left(\frac{\prod_{u\neq k}^{N} d_u}{d_k^{N-1}}\right) \mathrm{Perm}\left(\left(\boldsymbol{P}_k^{-1}\boldsymbol{Q}_k\right)\right). \tag{70}$$

The average asymptotic SER in (60) can then be calculated as

$$\mathrm{SER}_k^{\infty} \simeq \frac{\mathcal{I}_k(\boldsymbol{P},\boldsymbol{D})\mathrm{Perm}(\boldsymbol{Q}_k)}{|\boldsymbol{P}_k| d_k^L}\bar{\gamma}^{-L}, \quad \forall\, k, \tag{71}$$

where the integral $\mathcal{I}_k(\boldsymbol{P},\boldsymbol{D})$ is given in (25) and $\bar{\gamma} = 1/\sigma^2$.

$$\mathcal{I}_k(\boldsymbol{P},\boldsymbol{D}) = \frac{a}{\pi}\int_0^T \frac{\left(\prod_{u\neq k}^{N} \frac{d_u}{d_k}\right)\sin^{2n_R}\theta}{\sum_{i=0}^{N-1}\zeta_i g^{n_R-i}\sin^{2i}\theta} d\theta. \tag{72}$$

## Appendix B
## Proof of Linear Independancy of $\mathrm{SER}_k^{\infty}(\boldsymbol{d}^*)$

The average asymptotic SERs for $n_R = N = 2$ are given

$$\mathrm{SER}_1^{\infty}(\boldsymbol{d}) \simeq \frac{\kappa_1}{\pi}\int_0^T \frac{d_2 \sin^4\theta}{d_1^{n_R} g + d_1^{n_R-1} d_2 \tau_1 \sin^2\theta} d\theta, \tag{73}$$

$$\mathrm{SER}_2^{\infty}(\boldsymbol{d}) \simeq \frac{\kappa_2}{\pi}\int_0^T \frac{d_1 \sin^4\theta}{d_2^{n_R} g + d_2^{n_R-1} d_1 \tau_2 \sin^2\theta} d\theta, \tag{74}$$

where $\kappa_1 = \mathrm{Perm}(\boldsymbol{P}_2)\bar{\gamma}^{-L}/|\boldsymbol{P}_1|g^{n_R-1}$, $\kappa_2 = \mathrm{Perm}(\boldsymbol{P}_1)\bar{\gamma}^{-L}/|\boldsymbol{P}_2|g^{n_R-1}$, $\tau_1 = \mathrm{Perm}(\boldsymbol{P}_1^{-1}\boldsymbol{P}_2)$, and $\tau_2 = \mathrm{Perm}(\boldsymbol{P}_2^{-1}\boldsymbol{P}_1)$. From $\mathrm{SER}_1^{\infty}(\boldsymbol{d})$ and $\mathrm{SER}_2^{\infty}(\boldsymbol{d})$, it is straightforward to calculate partial derivatives, $\partial\mathrm{SER}_1^{\infty}(\boldsymbol{d})/\partial d_1$, $\partial\mathrm{SER}_1^{\infty}(\boldsymbol{d})/\partial d_2$, $\partial\mathrm{SER}_2^{\infty}(\boldsymbol{d})/\partial d_1$, and $\partial\mathrm{SER}_2^{\infty}(\boldsymbol{d})/\partial d_2$. Furthermore, it is easy to prove that

$$\frac{\partial\mathrm{SER}_1^{\infty}(\boldsymbol{d})}{\partial d_1}\frac{\partial\mathrm{SER}_2^{\infty}(\boldsymbol{d})}{\partial d_2} - \frac{\partial\mathrm{SER}_1^{\infty}(\boldsymbol{d})}{\partial d_2}\frac{\partial\mathrm{SER}_2^{\infty}(\boldsymbol{d})}{\partial d_1} > 0, \tag{75}$$

for all $\boldsymbol{d}$. It implies that $\nabla\mathrm{SER}_1^{\infty}(\boldsymbol{d}^*)$, and $\nabla\mathrm{SER}_2^{\infty}(\boldsymbol{d}^*)$ are linearly independent.

## Acknowledgment

We thank the anonymous reviewers for the helpful and constructive comments which have greatly helped to improve our manuscript.

## References

[1] G. Foschini, H. Huang, K. Karakayali, R. Valenzuela, and S. Venkatesan, "The value of coherent base station coordination," in *Proc. Conf. Inf. Sci. Syst.*, Baltimore, MD, USA, Mar. 2005, pp. 141–145.
[2] M. K. Karakayali, G. J. Foschini, and R. A. Valenzuela, "Network coordination for spectrally efficient communications in cellular systems," *IEEE Trans. Wireless Commun.*, vol. 13, no. 4, pp. 56–61, Aug. 2006.
[3] R. Irmer *et al.*, "Coordinated multipoint: Concepts, performance, field trial results," *IEEE Commun. Mag.*, vol. 13, no. 4, pp. 102–111, Feb. 2011.
[4] D. Gesbert, M. Kountouris, R. W. Heath, C. B. Chae, and T. Salzer, "Shifting the MIMO paradigm," *IEEE Signal Process. Mag.*, vol. 24, no. 5, pp. 36–46, Sep. 2007.
[5] *Coordinated Multi-Point Operation for LTE Physical Layer Aspects*, 3GPP TR 36.819 V11.1.0, Dec. 2011.
[6] Y. Liang, A. Goldsmith, G. Foschini, R. Valenzuela, and D. Chizhik, "Evolution of base stations in cellular networks: Denser deployment versus coordination," in *Proc. Int. Conf. Commun.*, Baltimore, MD, USA, May 2008, pp. 4128–4132.
[7] *Evolved Universal Terrestrial Radio Access (E-UTRA) Physical Layer Procedures*, 3GPP TS 36.213 V11.3.0, Jul. 2013.
[8] G. J. Foschini and Z. Miljanic, "A simple distributed autonomous power control algorithm and its convergence," *IEEE Trans. Veh. Technol.*, vol. 42, no. 4, pp. 641–646, Nov. 1993.
[9] R. D. Yates, "A framework for uplink power control in cellular radio system," *IEEE J. Sel. Areas Commun.*, vol. 13, no. 7, pp. 1341–1347, Sep. 1995.
[10] R. Chen, J. G. Andrews, R. W. Heath, Jr., and A. Ghosh, "Uplink power control in multi-cell spatial multiplexing wireless systems," *IEEE Trans. Wireless Commun.*, vol. 6, no. 7, pp. 2700–2711, Jul. 2007.
[11] D. A. Basnayaka, P. J. Smith, and P. A. Martin, "Performance analysis of macrodiversity MIMO systems with MMSE and ZF receivers in flat Rayleigh fading," *IEEE Trans. Wireless Commun.*, vol. 12, no. 5, pp. 2240–2251, May 2013.
[12] A. Goldsmith, *Wireless Communications*. Cambridge, U.K.: Cambridge Univ. Press, 2005.
[13] S. Verdú, *Multiuser Detection*. Cambridge, U.K.: Cambridge Univ. Press, 1998.
[14] *Uplink Coordinated Multi-Point Reception With Distributed Inter-Cell Interference Suppression for LTE-A*, 3GPP R1-090770, Feb. 2009.
[15] L. Dai, "A comparative study on uplink sum capacity with co-located and distributed antennas," *IEEE J. Sel. Areas Commun.*, vol. 29, no. 6, pp. 1200–1213, Jun. 2011.
[16] F. Diehm, G. Chen, and G. Fettweis, "Power control and scheduling for joint detection cooperative cellular systems," in *Proc. IEEE GLOBECOM*, Anaheim, CA, USA, Dec. 2012, pp. 4012–4017.
[17] S. Hanly, "Capacity and power control in spread spectrum macrodiversity radio networks," *IEEE Trans. Commun.*, vol. 44, no. 2, pp. 247–256, Feb. 1996.
[18] T. S. Rappaport *et al.*, "Millimeter wave mobile communications for 5G cellular: It will work!" *IEEE Access*, vol. 1, pp. 335–349, May 2013.
[19] S. Haykin, *Adaptive Filter Theory*, 4th ed. Upper Saddle River, NJ, USA: Prentice Hall, 2001.

[20] J. H. Winters, "Optimum combining in digital mobile radio with co-channel interference," *IEEE J. Sel. Areas Commun.*, vol. SAC-2, no. 4, pp. 528–539, Jul. 1984.
[21] D. A. Basnayaka, P. J. Smith, and P. A. Martin, "Ergodic sum capacity of macrodiversity MIMO systems in flat Rayleigh fading," *IEEE Trans. Inf. Theory*, vol. 59, no. 9, pp. 5257–5270, Sep. 2013.
[22] H. Minc, *Permanants,* 1st ed. Reading, MA, USA: Addison-Wesley, 1978.
[23] I. S. Gradshteyn and I. M. Ryzhik, *Table of Integrals, Series, Products,* 6th ed. Boston, MA, USA: Academic, 2000.
[24] W. Yu, W. Rhee, S. Boyd, and J. Cioffi, "Iterative water-filling for Gaussian vector multiple-access channels," *IEEE Trans. Inf. Theory*, vol. 50, no. 1, pp. 145–152, Jan. 2004.
[25] S. Kandukuri and S. Boyd, "Optimal power control in interference-limited fading wireless channels with outage-probability specifications," *IEEE Trans. Wireless Commun.*, vol. 1, no. 1, pp. 46–55, Jan. 2002.
[26] J. Y. Kim, G. L. Stber, and I. F. Akyildiz, "Macrodiversity power control in hierarchical CDMA cellular systems," *IEEE J. Sel. Areas Commun.*, vol. 19, no. 2, pp. 266–276, Feb. 2001.
[27] S. Boyd and L. Vandenberghe, *Convex Optimization*. Cambridge, U.K.: Cambridge Univ. Press, 2004.
[28] A. Edelman and H. Murakami, "Polynomial roots from companion matrix eigenvalues," *Math. Comput.*, vol. 64, no. 210, pp. 763–776, Apr. 1995.
[29] D. Cruz-Uribe and C. J. Neugebauer, "An elementary proof of error estimates for the trapezoidal rule," *Math. Mag.*, vol. 76, no. 4, pp. 303–306, Oct. 2003.
[30] E. Larsson, O. Edfors, F. Tufvesson, and T. Marzetta, "Massive MIMO for next generation wireless systems," *IEEE Commun. Mag.*, vol. 52, no. 2, pp. 186–195, Feb. 2014.
[31] C. G. Broyden, "A class of methods for solving nonlinear simultaneous equations," *Math. Comput.*, vol. 19, pp. 577–593, 1965.

**Dushyantha A. Basnayaka** (S'11–M'12) received the B.Sc.Eng. degree with first-class honors from the University of Peradeniya, Kandy, Sri Lanka, in 2006 and the Ph.D. degree in electrical engineering from the University of Canterbury (UC), Christchurch, New Zealand, in 2012.

From 2006 to 2009, he was a System Engineer at MillenniumIT (a member company of London Stock Exchange group). From 2009 until 2012, he was with the Communication Research Group, UC. Since 2013, he has been a Research Fellow in wireless communication with the University of Edinburgh, Edinburgh, U.K. His current research interests include massive multiple-input multiple-output (MIMO), spatial modulation, interference mitigation techniques for cellular wireless systems, and macrodiversity multiuser-MIMO systems.

Dr. Basnayaka was a recipient of the UC International Doctoral Scholarship for his doctoral studies.

**Harald Haas** (S'98–A'00–M'03) is the Chair of Mobile Communications with the Institute for Digital Communications (IDCOM), University of Edinburgh, Edinburgh, U.K., and he is currently the Chief Scientific Officer of a university spin-out company pureVLC Ltd. He holds 23 patents. He has published more than 60 journal papers, including a science article, and more than 160 peer-reviewed conference papers, and nine of his papers are invited papers. He has coauthored a book entitled "Next Generation Mobile Access Technologies: Implementing TDD" with Cambridge University Press. Since 2007, he has been a Regular High-Level Visiting Scientist supported by the Chinese 111 program at the Beijing University of Posts and Telecommunications (BUPT), Beijing, China. His main research interests include interference coordination in wireless networks, spatial modulation, and optical wireless communication. He was an Invited Speaker at the TED Global Conference 2011, and his work on optical wireless communication was listed among the "50 best inventions in 2011" in Time Magazine. He recently has been awarded a prestigious Fellowship of the Engineering and Physical Sciences Research Council (EPSRC) in the U.K.